IMA Journal of Mathematics Applied in Business & Industry (1999) **10**, 55–86

A mathematical model for the heat treatment of glass fabric sheets

A. BUIKIS
Institute of Mathematics, Latvian Academy of Sciences and University of Latvia, 1, Akademijas l., LV-1524 Riga, Latvia

A. D. FITT
Faculty of Mathematical Studies, University of Southampton, Southampton SO17 1BJ, England

[Received 17 June 1997 and in revised form 18 March 1998]

During the industrial process of glass fabric manufacture in Latvia, an oil that has earlier been added to the fabric must be removed. To accomplish this, the fabric is passed through a furnace where the oil is removed by burning. It is known that the oil removal process reduces the tensile strength of the fabric. The burning process is analysed via a simple mathematical model that allows the furnace parameters to be optimized. Using some of the well-established properties of glass, it is shown that it is the cooling rather than the heating process that adversely affects the final product. A thermoviscoelastic model is developed to predict the permanent stress in the glass fabric. Some suggestions for modifications to the process are also examined, and it is shown that, to a large extent, the strength of the fabric may be preserved without significantly adding to the cost or intricacy of the production process.

1. Introduction

This study concerns the optimization of a process for producing a glass fabric Such fabrics are used for protective, electrical, and thermal insulation and decorative purposes. The particular product that is discussed below is manufactured at the Valmiera Glass Fibre Plant in Valmiera, Latvia.

The glass fabric may be thought of as a woven material, individual glass fibres forming the 'thread' of the fabric. The glass threads that are used are extremely small (typically 6–9 μ), and a typical sample of fabric has a thickness of about 0.2 mm. During the initial stages of the manufacture of glass threads and the weaving of the fabric, it is necessary to add oil to the glass in order to form the required product. Once the weaving is complete, however, the oil is no longer required. The oil itself occupies only about 1 per cent by mass of the woven glass fabric, and, were it not for its chemical properties, could safely remain permanently in the fabric. A number of reasons, however, make it essential that the oil is removed. Firstly, the efficiency of the fabric as a thermal and electrical insulator would be severely compromised by the presence of oil. Secondly, the oil blackens the fabric, and for decorative purposes the fabric is required to be white. The fabric is therefore unusable unless the oil can be removed. For the purposes of the following discussion, it may be assumed that, to make a commercially successful product, the oil must be reduced in volume fraction to a 'safe' level of about 0 05 per cent.

In order to remove the oil, the fabric is pulled through a furnace (see Fig. 1 for a schematic diagram). The furnace chamber is 1166 mm long, 1430 mm wide, and has a

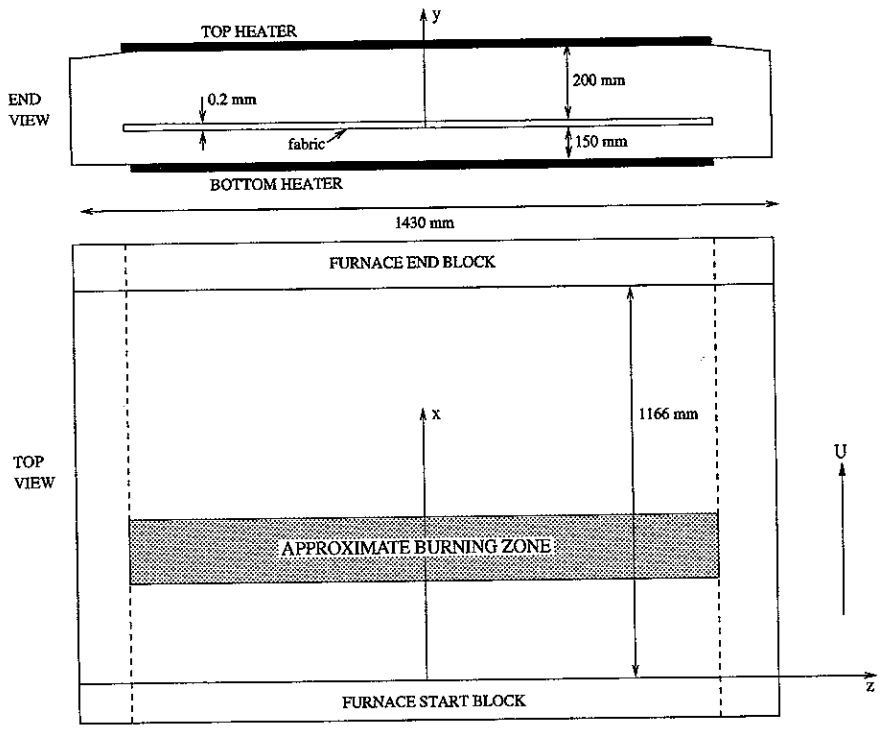

FIG 1 Schematic diagram (not to scale) of furnace, fabric, and heaters.

height of about 350 mm. Heat is provided by diesel-fuel-powered elements situated at the top and bottom of the furnace (see diagram) Further details of the heating process will be given in the next section, but the basic intention is that the fabric should be heated to a sufficient temperature so that the oil burns and is therefore removed. It is worth noting that, under normal operating conditions, most of the oil is expected to burn away in a fairly short 'burning zone'. However, even when this has happened, some isolated spots of oil remain in the fabric. It is therefore essential that the furnace exit is placed some distance from the end of the 'burning zone' so that these remaining impurities may be removed.

Underneath the burning zone, a pipe is placed in the furnace. The pipe has a large number of holes, and air is blown into the pipe from outside the furnace. This arrangement has two advantages; firstly it assists the combustion process, and secondly it provides a constant throughput of air to allow combustion products to be removed at the entrance and exit to the furnace. (It is possible that changes to the models presented below should be made to account for the effect of this air on the combustion zone. In the factory, however, the air injection is regarded more as a means of removing pollutants than as a way of enhancing combustion. In the absence of any firm data, therefore, its effect on the burning zone has necessarily been ignored.)

Evidently the parameters of the furnace (for example, the pull-through speed of the

fabric and the properties of the heating elements) need to be optimized in order to ensure that a sufficient amount of oil is removed from the fabric using as little energy as possible, but in addition to this there is a further effect that must be considered: it is known that the oil removal process adversely affects the tensile strength of the glass fabric. The real challenge therefore is to minimize the loss of tensile strength in the material as well as minimize the energy required to burn away the oil. In order to discuss this problem completely, we shall see that the fate of the glass fabric after it has left the furnace region needs to be carefully analysed; at present the fabric simply exits into air at room temperature. Once the process by which the fabric loses strength has been understood, it is possible to pose some plausible (and economically viable) possibilities for improving the process.

2. A mathematical model of the furnace

We begin by proposing a simple mathematical model for the behaviour of the glass fabric inside a furnace. For convenience, a list of the notation used is provided in the appendix. Using the coordinate system given in Fig. 1 we assume that the fabric occupies the region $\{0 \leqslant x \leqslant L, 0 \leqslant y \leqslant \delta, 0 \leqslant z \leqslant D\}$ in the furnace and is drawn through the furnace in the x direction with constant speed U. In reality, fabric sheets of width $D = 1.1$ m and thickness $\delta = 0.2$ mm are used; we therefore neglect variations in the z direction. The temperature distribution in the fabric at a cross-section z = constant satisfies

$$\rho c_p \left(\frac{\partial \tilde{T}}{\partial t} + U \frac{\partial \tilde{T}}{\partial x} \right) = \frac{\partial}{\partial x} \left(k \frac{\partial \tilde{T}}{\partial x} \right) + \frac{\partial}{\partial y} \left(k \frac{\partial \tilde{T}}{\partial y} \right) + \tilde{R}_1, \tag{1}$$

where ρ and c_p denote respectively the density and specific heat of the glass fabric, k is the thermal conductivity, and $\tilde{T}$ is the fabric temperature. The term $\tilde{R}_1$, as yet unspecified, denotes the heating sources arising from chemical reactions and any other effects that may occur in the fabric.

Some approximations have implicitly been made in (1). Strictly speaking, since the fabric contains a small amount of oil, the thermal constants should take into account the properties of the oil. Thus, for example, we should write (given that the dependence is linear—a large assumption in itself) $\tilde{k} = k + k_o c$ where k_o denotes the thermal conductivity and c the concentration of the oil. Because the oil concentration never exceeds about 1 per cent (by mass) of the fabric, however, variations in ρ, c_p, and k due to the presence of the oil have been neglected. The equation (1) also assumes that the amalgam of glass rods and air that constitutes the fabric behaves as an 'ordinary' conductor. Since the time scale for diffusion across a 10 μ air gap is around 10^{-5} seconds and the flow through the fabric is negligible, this seems an entirely reasonable assumption.

Before proceeding further, we note that, since distances in the y direction are typically of order $\delta = 0.2$ mm, while $k = 1.38$ W/m/K, $\rho = 1100$ kg/m^3, and $c_p = 690.82$ J/kg/K, and the y diffusion time scale in the glass fabric is of order $\rho c_p \delta^2 / k \sim 2 \times 10^{-2}$ sec. Usually the fabric speed U is of order 20 m/min $\sim$ 0.33 m/sec, and the furnace heater length is $L = 1.166$ m; the residence time in the furnace is thus typically 3 5 sec, and so heat is transferred from the fabric surface to its interior extremely quickly after it has entered the

furnace. We therefore work from now on in terms of an average temperature defined by

$$T(x,t) = \frac{1}{\delta}\int_0^{\delta} \tilde{T}(x,y,t)\,\mathrm{d}y.$$

Having integrated (1), we obtain

$$\rho c_p\left(\frac{\partial T}{\partial t} + U\frac{\partial T}{\partial x}\right) = \frac{\partial}{\partial x}\left(k\frac{\partial T}{\partial x}\right) + \frac{1}{\delta}\left[k\frac{\partial \tilde{T}}{\partial y}(x,\delta,t) - k\frac{\partial \tilde{T}}{\partial y}(x,0,t)\right] + R_1 \qquad (2)$$

Before further simplifications are performed on (2), we will consider the boundary conditions that describe the external mechanisms such as the radiation from the heaters and the convection arising from the air pipe underneath the burning zone. Assuming first of all that radiative heat transfer of the simplest possible type takes place, on the top side of the fabric where $y = \delta$, we have

$$k\frac{\partial \tilde{T}}{\partial y} = \epsilon_f\sigma(T_{ht}^4 - \tilde{T}^4) + \alpha(\tilde{T})(T_g - \tilde{T}). \qquad (3)$$

Here ϵ_f is the fabric emissivity, σ is the Stefan–Boltzmann constant, T_{ht} is the temperature (assumed constant) of the heater at the furnace top surface, T_g is the temperature of the gas in the furnace, and α is the convective heat transfer coefficient. Complicated models for α may be proposed; for the current purposes we simply assume that (see, for example Miheev (1940))

$$\alpha(T) = \mathrm{Nu}\frac{k_g}{L},$$

where the Nusselt number Nu is defined in terms of the gas Reynolds number $\mathrm{Re} = LU_g/\nu_g$ by

$$\mathrm{Nu} = 0.044\mathrm{Re}^{0.77}\frac{T}{T_g},$$

and U_g, ν_g, and k_g are respectively the velocity, kinematic viscosity, and thermal conductivity of the furnace gas. We shall assume that Re, k_g, and ν_g are simply given; in reality they depend on temperature, so that, for example for $T_g = 720°\mathrm{C}$, we have $k_g = 0\ 0669$ W/m/K and $\nu_g = 1.20 \times 10^{-4}\,\mathrm{m}^2/\mathrm{sec}$, while for $T_g = 30°\mathrm{C}$ the relevant values are $k_g = 0.0258\mathrm{W/m/K}$ and $\nu_g = 0.166 \times 10^{-4}\,\mathrm{m}^2/\mathrm{sec}$. As far as the gas flow rate is concerned, the entrance and exit to the furnace are relatively narrow. It therefore seems plausible that much of the air from the pipe beneath the burning zone is convected with the fabric. In the absence of any firm experimental data, we assume that $U_g \sim U = 0.33\,\mathrm{m/sec}$.

For the boundary condition at the bottom surface $y = 0$ of the fabric, arguments similar to those used for (3) apply, giving

$$-k\frac{\partial \tilde{T}}{\partial y} = \epsilon_f\sigma(T_{hb}^4 - \tilde{T}^4) + \alpha(\tilde{T})(T_g - \tilde{T}), \qquad (4)$$

where T_{hb} is the temperature of the heater on the furnace bottom.

The expressions (3) and (4) may now be substituted into equation (2). Further assuming that $\tilde{T}(x, y, t)$ is constant in y (see later section for equations appropriate for thicker fabrics) for a given x and t, so that $\tilde{T}(x, y, t) = T(x, t)$, we find that

$$\rho c_p \left(\frac{\partial T}{\partial t} + U \frac{\partial T}{\partial x} \right) = \frac{\partial}{\partial x} \left(k \frac{\partial T}{\partial x} \right) + \frac{\epsilon_f \sigma}{\delta} (T_{ht}^4 + T_{hb}^4 - 2T^4) + \frac{2\alpha(T)}{\delta} (T_g - T) + R_1. \quad (5)$$

Until now, possible contributions from reflected radiation have been ignored in the boundary conditions (3) and (4). The distances between the fabric surfaces and the heaters on the top and bottom of the furnace are 200 mm and 150 mm respectively, while the heater temperatures are typically $T_{ht} = 700°C$ and $T_{hb} = 850°C$. We may expect, therefore, that the impact of reflected radiation will be greater from the bottom of the furnace. (It is not easy to estimate a priori how much more important the contributions from the bottom will be; our approach will be simply to ignore reflected radiation from the top surface. The justification of this comes mainly from the results contained later in the paper.) If the effects of reflected radiation are to be included, the boundary condition (4) must be modified. Consider the fabric surface; then if J_f and G_f denote respectively the radiosity (radiation leaving the fabric surface per unit time per unit area) and irradiation (radiation incident on the fabric per unit time per unit area), and r_f denotes the total fabric reflectivity, we have, in the absence of transmission, $r_f + \epsilon_f = 1$ and therefore, taking a reflection into account,

$$J_f = \sigma \epsilon_f \tilde{T}^4 + r_f G_f. \quad (6)$$

The net energy Q_f leaving the fabric surface is

$$Q_f = J_f - G_f = \sigma \epsilon_f \tilde{T}^4 - \epsilon_f \left[\frac{J_f - \sigma \epsilon_f \tilde{T}^4}{1 - \epsilon_f} \right].$$

The boundary condition (4) thus becomes

$$-k \frac{\partial \tilde{T}}{\partial y} = \frac{\epsilon_f}{1 - \epsilon_f} (J_f - \sigma \tilde{T}^4) + \alpha(\tilde{T})(T_g - \tilde{T}) \quad (7)$$

As yet, J_f is unknown. However, from (6) we know that J_f is given in terms of T and G_f. The net irradiation G_f at any point on the fabric arises from contributions from all points on the heater. Using an elementary geometrical argument (see Siegel & Howell (1972) for further details) thus gives

$$J_f(x, t) = \epsilon_f \sigma \tilde{T}^4(x, 0, t) + (1 - \epsilon_f) \int_0^L J_h(\xi, t) \frac{a^2}{2((\xi - x)^2 + a^2)^{3/2}} \, d\xi,$$

where J_h is the heater radiosity. Accounting for a reflection from the heater in exactly the same manner as from the fabric, the heater radiosity must satisfy

$$J_h(x, t) = \epsilon_h \sigma T_{hb}^4 + (1 - \epsilon_h) \int_0^L J_f(\xi, t) \frac{a^2}{2((\xi - x)^2 + a^2)^{3/2}} \, d\xi,$$

where ϵ_h is the heater emissivity and a is the distance between the bottom heater and the fabric.

Some more attention will be given below to the properties of the oil, and for the present we assume simply that, when the oil burns, it does so via a simple one-step Arrhenius reaction with activation energy E_a, the energy release being proportional to the concentration c of oil (measured in mol/m^3) remaining at any particular time and position in the fabric. The equations thus become (in the absence of reflected radiation)

$$\rho c_p\left(\frac{\partial T}{\partial t}+U\frac{\partial T}{\partial x}\right)=k\frac{\partial^2 T}{\partial x^2}+\frac{\epsilon_f\sigma}{\delta}(T_{ht}^4+T_{hb}^4-2T^4)+\frac{2\alpha(T)}{\delta}(T_g-T)+c\Delta HA\exp(-E_a/RT)$$

$$\frac{\partial c}{\partial t}+U\frac{\partial c}{\partial x}=-cA\exp(-E_a/RT),$$

or, when the effects of reflected radiation are included,

$$\rho c_p\left(\frac{\partial T}{\partial t}+U\frac{\partial T}{\partial x}\right)=k\frac{\partial^2 T}{\partial x^2}+\frac{\epsilon_f}{\delta}\left[\sigma(T_{ht}^4-T^4)+\frac{1}{1-\epsilon_f}(J_f-\sigma T^4)\right]+$$

$$\frac{2\alpha(T)}{\delta}(T_g-T)+c\Delta HA\exp(-E_a/RT),$$

$$\frac{\partial c}{\partial t}+U\frac{\partial c}{\partial x}=-cA\exp(-E_a/RT),$$

$$J_f(x,t)=\epsilon_f\sigma T^4(x,t)+(1-\epsilon_f)\int_0^L J_h(\xi,t)\frac{a^2}{2((\xi-x)^2+a^2)^{3/2}}\,d\xi,$$

$$J_h(x,t)=\epsilon_h\sigma T_{hb}^4+(1-\epsilon_h)\int_0^L J_f(\xi,t)\frac{a^2}{2((\xi-x)^2+a^2)^{3/2}}\,d\xi$$

Here A is a pre-exponential Arrhenius constant, ΔH is the heat of combustion of the oil, and R the gas constant.

Some comments on these two models are in order; In the first model, the unknowns are T and c, and the boundary conditions are that T is given at the entrance to the furnace and T_x is zero at the (insulated) exit to the furnace, c is given at the entrance to the furnace, and initial distributions of T and c are given.

When reflected radiation is included, the unknowns are now T, c, J_f, and J_h. The boundary and initial conditions, however, are identical to the previous case since, if the temperature is known at $t = 0$, the two integral equations may be solved to yield $J_f(x, 0)$ and $J_h(x, 0)$.

2.1 *Non-dimensionalization of the equations*

In order to determine the relative importance of terms in the equations, a non-dimensionalization may be performed. Considering for simplicity the equations where reflected radiation is ignored (the inclusion or otherwise of reflected radiation evidently changes the quantitative results, but cannot affect the orders of magnitude involved) we set $x = L\bar{x}$,

$t = L\bar{t}/U$, $T = T_{hb}\theta$, and $c = c_0\bar{c}$, where c_0 is the initial concentration of oil in the fabric. On dropping the bars, the equations then become

$$\frac{\partial\theta}{\partial t}+\frac{\partial\theta}{\partial x} = N_1\frac{\partial^2\theta}{\partial x^2}+N_2\left[\left(\frac{T_{ht}}{T_{hb}}\right)^4+1-2\theta^4\right]+N_3\left(\frac{T_g}{T_{hb}}-\theta\right)+N_5 c\exp(-N_4(1-\theta)/\theta),$$

$$\frac{\partial c}{\partial t}+\frac{\partial c}{\partial x} = -N_6 c\exp(-N_4(1-\theta)/\theta),$$

where

$$N_1 = \frac{k}{L\rho U c_p}, \qquad N_2 = \frac{\sigma\epsilon_f L T_{hb}^3}{\rho U c_p \delta}, \qquad N_3 = \frac{2L\alpha(T)}{\rho U c_p \delta},$$

$$N_4 = \frac{E_a}{RT_{hb}}, \qquad N_5 = \frac{c_0 L\,\Delta\, HA}{\rho U c_p T_{hb}}\exp(-E_a/RT_{hb}), \qquad N_6 = \frac{LA}{U}\exp(-E_a/RT_{hb})$$

Using the values of the constants given in the nomenclature table, (and assuming for simplicity that α is evaluated when $T = T_g$) we find that

$$N_1 \sim 4.7\times 10^{-6}, \qquad N_2 \sim 1.72, \qquad N_3 \sim 0\,06,$$

$$N_4 \sim 17.14, \qquad N_5 \sim 51.26, \qquad N_6 \sim 128.68.$$

Some simple conclusions may be drawn from these results; first, the diffusion in the x direction is negligible and will be ignored. (In this case the boundary condition at the furnace exit is no longer required.) Secondly, since N_5 is sizeable, it transpires that the combustion reaction makes a non-negligible contribution to the overall heat balance within the furnace, and must be included in the energy equation. Finally, the size of N_4 suggests that a high-activation-energy approach may be possible, though we do not pursue this further here.

A comment regarding flow in the glass is also in order. When the thermal properties of glass are discussed in more detail in the next section, it will emerge that the furnace operating temperature is well above the melting point of glass. The question therefore arises as to whether significant viscous flow can take place in the glass. To answer this, we consider the slow viscous flow, under gravity, of a single fibre filament of radius $h =$ 0 1 mm say. Flow can only take place if the pressure and viscous forces in Stokes' equations are balanced by the gravitational body force term; thus if V $(= h/\tau)$ denotes velocity, and τ is a typical time taken for the glass to 'slump' an order of magnitude distance h under its own weight, we must have

$$\frac{\mu V}{\rho h^2} \sim g.$$

Hence the time scale for appreciable flow in the fabric is given by $\tau \sim \nu/hg$. To obtain a 'worst-case' estimate, we consider glass at 1300°C and use the data for KG-33 Borosilicate (one of the less viscous glasses at this temperature). This has a dynamic viscosity of about 500 N/s/m^2, giving $\tau \sim 625$ sec. Flow in the glass may therefore be discounted.

2.2 *Properties of the oil*

Before solutions to the models described above may be obtained, the relevant physical constants must be identified. Owing to the chemical complexity of the substances involved, this is a non-trivial matter. The chemical formula for the oil is known to be $C_{22}H_{46}N_3O_7$, and the burning reaction proceeds via

$$C_{22}H_{46}N_3O_7 + 31.5O_2 \rightarrow 22CO_2 + 23H_2O + 3NO$$

The chemical and combustion properties of oils are not easy to determine. The factory at Valmiera has conducted experiments that suggest that the ignition temperature of the oil is given by $T_{io} = 420°C$. For the heat of combustion ΔH of the oil we rely again on data provided by the Valmiera factory, the recommended value being 2.596×10^7 J/kg = 1.207×10^7 J/mol. As far as the activation energy is concerned, although detailed information is not available, E_a does not change a great deal for a large range of oils; Brandrup *et al.* (1975) suggest a value of 170–200 kJ/mol, and, based on some other values available for oils, we assume that in this case $E_a = 160$ kJ/mol.

To determine the initial concentration c_0 of oil in the fabric, we assume that a standard calculation may be used to determine the molecular weight of the oil. This gives 0.465 kg/mol. Assuming that before burning commences the fabric contains 1.2 per cent oil by weight, then (assuming that $\rho_o = 1100\,\text{kg/m}^3$) gives $c_0 = 28.387\,\text{mol/m}^3$.

Because of the difficulty of obtaining reliable values for the required constants, it is important to indicate the likely error involved. For the initial concentration, the activation energy, and the heat of combustion, it is possible to be fairly sure that, while the values used may contain errors, they are certainly correct to within an order of magnitude. We also note that, under general conditions, the mechanisms by which heated waxes and oils burn are extremely complex and may involve evaporation, separation of volatiles, and many other sub-processes. These possibilities have not been catered for in the analysis. As far as the pre-exponential Arrhenius constant is concerned, data are very hard to obtain, and the best that we have been able to do is to take a rough average based on the properties of 'similar' materials, arriving at a value of $A = 1.0 \times 10^9$/sec.

3. Temperature predictions in the fabric

The models proposed in the last section now allow the temperature of the fabric and the concentration of oil to be predicted. Although the start-up and wind-down processes may be of some interest, for the most part the process runs continuously, so that any dependence on time may be ignored.

3.1 *Predictions with no reflected radiation*

In order to determine the details of the oil removal process according to the simple model, it is necessary to solve the (dimensional) ordinary differential equations

$$\rho c_p U \frac{dT}{dx} = \frac{\epsilon_f \sigma}{\delta}(T_{ht}^4 + T_{hb}^4 - 2T^4) + \frac{2\alpha(T)}{\delta}(T_g - T) + c\Delta HA \exp(-E_a/RT), \quad (8)$$

$$U\frac{dc}{dx} = -cA \exp(-E_a/RT), \quad (9)$$

with

$$T(0) = T_0, \qquad c(0) = c_0.$$

Here T_0 denotes the ambient temperature of the fabric before it passes into the furnace.

Although it is not possible to determine a closed-form solution to the equations (8) and (9), solutions may easily be obtained using standard library routines. (In this instance, the MAPLE (version 2) routine 'dsolve,numeric' was used. This employs a Fehlberg 4th–5th order Runge–Kutta method. All computations were carried out out on a Sun SPARC2).

3.2 *Predictions when reflected radiation is included*

For the steady case with reflected radiation, the equations are

$$\rho c_p U \frac{dT}{dx} = \frac{\epsilon_f}{\delta}\left[\sigma(T_{ht}^4 - T^4) + \frac{1}{1-\epsilon_f}(J_f - \sigma T^4)\right] + \frac{2\alpha(T)}{\delta}(T_g - T) + c\,\Delta\, HA\exp(-E_a/RT) \tag{10}$$

$$U\frac{dc}{dx} = -cA\exp(-E_a/RT), \tag{11}$$

$$J_f(x) = \epsilon_f\sigma T^4(x) + (1-\epsilon_f)\int_0^L J_h(\xi)\frac{a^2}{2((\xi-x)^2+a^2)^{3/2}}\,d\xi, \tag{12}$$

$$J_h(x) = \epsilon_h\sigma T_{hb}^4 + (1-\epsilon_h)\int_0^L J_f(\xi)\frac{a^2}{2((\xi-x)^2+a^2)^{3/2}}\,d\xi \tag{13}$$

These must be solved subject to the boundary conditions $T(0) = T_0$, $c(0) = c_0$ Since an iterative method of some kind will clearly be required, it is worth giving some thought to the most efficient way of solving the ordinary differential equations that arise. Writing the differential equations as $y' = f(y)$, we may estimate the eigenvalues of the Jacobian $\partial f/\partial y$. Using values for T and c at various x stations from the results of the previous section, we find that the ratio of these eigenvalues can attain values of order 10^5, and hence the differential equations (as is commonly the case with problems involving chemical reactions) are stiff. When reflected radiation is ignored, this does not present practical problems, since (8) and (9) have to be solved only once, and efficient and accurate solutions may be obtained using standard methods with very small time steps. When (12) and (13) must be solved as well, however, an iterative scheme is necessary, and backward differentiation formulae (BDF) are required. The NAG routine D02EAF was therefore used. This is designed specifically for stiff first-order systems and uses a VSVO method implementing BDF. (For further details see Hall & Watt (1976).)

The equations (10)–(13) may now be solved using a straightforward iterative method; beginning with initial estimates for the functions $J_f(x)$ and $J_h(x)$, (in the calculations reported below, both were initially assumed to take the value $\epsilon_f\sigma T_{hb}^4$) the two ordinary differential equations (10) and (11) are solved numerically to obtain new estimates of c and T. Assuming thereafter that J_f and J_h are piecewise constant on intervals $[x_n, x_{n+1})$ where

$x_n = n\Delta x$ ($n \leqslant N$) and the interval $[0, L]$ has been divided into subintervals of width Δx, a simple trapezium-rule approximation shows that (12) and (13) may be approximated by

$$J_f(x_n) = \epsilon_f \sigma T^4(x_n) + (1 - \epsilon_f) \sum_{j=0}^{N-1} \left(\frac{J_h(x_{j+1}) + J_h(x_j)}{2} \right) [g(x_{j+1}, x_n) - g(x_j, x_n)],$$

$$J_h(x_n) = \epsilon_h \sigma T_{hb}^4 + (1 - \epsilon_h) \sum_{j=0}^{N-1} \left(\frac{J_f(x_{j+1}) + J_f(x_j)}{2} \right) [g(x_{j+1}, x_n) - g(x_j, x_n)],$$

where

$$g(x_j, x_n) = \frac{x_j - x_n}{2\sqrt{(x_j - x_n)^2 + a^2}}.$$

It is worth pointing out that many more-sophisticated schemes may be developed by using higher-order integration rules. For our purposes, however, the scheme described above proved to be satisfactory. Lack of space precludes any detailed analysis of this method, but in all cases convergence was achieved after around 100 iterations. The usual comparisons for different numbers of mesh points indicated that the method was giving consistent and accurate results when 100–200 mesh points were used.

3.3 *Results*

It should be noted that, in all results given here, the emissivity of the fabric was taken to be 0.92. Originally, engineers from the Valmiera factory estimated that the fabric emissivity was between 0.4 and 0.6, a result partly motivated by the white appearance of the fabric. If computations are carried out with these values, however, it soon becomes clear that the fabric does not reach the temperatures that are observed. Because of this fact, separate experiments were carried out at the University of Latvia in Riga to determine ϵ_f. These indicated that a value of 0.92 was much more realistic, and so, in spite of its appearance, the fabric behaves more like an ideal *black* body. This is primarily because of the porous nature of the fabric. Further numerical experiments (for details see Buikis *et al.* (1997)) may be performed to show that the temperature is very sensitive to the value of the fabric emissivity that is assumed.

Figure 2 shows typical results for the model with no reflected radiation. Using the parameter values given in the appendix, we find that the fabric temperature rises to a maximum of about 1350 K before falling to a constant value. (This constant value, given by $T \sim 1056$ K, can of course be calculated simply by solving the quartic equation which results when all derivatives and the oil concentration c are set to zero in (8)) The oil concentration remains virtually constant before falling to zero over a 'burning zone' which approximately occupies the region 0.25–0.32 m. These predictions are generally in accord with observations made at the factory, and confirm that, with the parameter values currently used in the process, there is time for any remaining oil blemishes to be burned out of the fabric before the furnace exit.

The fact that the fabric emissivity ~ 1 may be used to provide a check on the numerical solutions to (10)–(13). Although in all cases the numerical scheme seemed to be producing

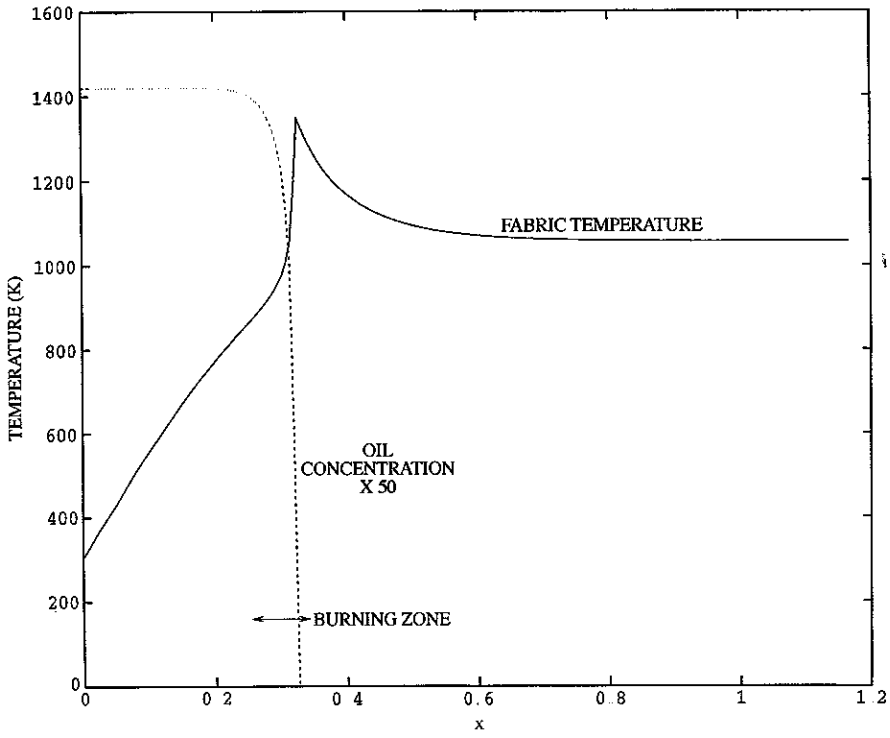

FIG 2. Fabric temperature and oil concentration for model with no reflected radiation.

credible results, confidence in the predictions may be increased by non-dimensionalizing (12) and (13). Setting $x = L\bar{x}$, $T = T_{\mathrm{hb}}\theta$, $J_{\mathrm{f}} = \sigma T_{\mathrm{hb}}^4 \bar{J}_{\mathrm{f}}$, and $J_{\mathrm{h}} = \sigma T_{\mathrm{hb}}^4 \bar{J}_{\mathrm{h}}$, we find that

$$\bar{J}_{\mathrm{f}}(\bar{x}) = \epsilon_{\mathrm{f}}\theta^4 + (1-\epsilon_{\mathrm{f}}) \int_0^1 \bar{J}_{\mathrm{h}}(\bar{\xi}) K(\bar{\xi}, \bar{x})\, \mathrm{d}\bar{\xi},$$

$$\bar{J}_{\mathrm{h}}(\bar{x}) = \epsilon_{\mathrm{h}} + (1-\epsilon_{\mathrm{h}}) \int_0^1 \bar{J}_{\mathrm{f}}(\bar{\xi}) K(\bar{\xi}, \bar{x})\, \mathrm{d}\bar{\xi},$$

where

$$K(\bar{\xi}, \bar{x}) = \frac{b^2}{2((\bar{\xi}-\bar{x})^2 + b^2)^{3/2}} \qquad (b = a/L).$$

If we now assume that $\epsilon_{\mathrm{f}} = 1-\epsilon$ and $\epsilon_h = 1 - s\epsilon$, where $\epsilon \ll 1$ and $s = O(1)$, then using regular perturbation expansions

$$\bar{J}_{\mathrm{f}} = \bar{J}_{\mathrm{f0}} + \epsilon \bar{J}_{\mathrm{f1}} + \epsilon^2 \bar{J}_{\mathrm{f2}} + \cdots, \qquad \bar{J}_{\mathrm{h}} = \bar{J}_{\mathrm{h0}} + \epsilon \bar{J}_{\mathrm{h1}} + \epsilon^2 \bar{J}_{\mathrm{h2}} + \cdots,$$

we find, on inserting the expression for $\bar{J}_{\mathrm{h}}$ into the integral equation for $\bar{J}_{\mathrm{f}}$, that

$$\bar{J}_{\mathrm{f0}}(\bar{x}) = \theta^4(\bar{x}), \qquad \bar{J}_{\mathrm{f1}}(\bar{x}) = -\theta^4(\bar{x}) + g_1(\bar{x}),$$

and

$$\bar{J}_{f2}(\bar{x}) = -sg_1(\bar{x}) + s\int_0^1 \theta^4(\bar{x}_1)g_2(\bar{x},\bar{x}_1)\,d\bar{x}_1,$$

where

$$g_1(\bar{x}) = \int_0^1 K(\bar{\xi},\bar{x})\,d\bar{\xi} = g(1,\bar{x}) - g(0,\bar{x}) = \frac{1-\bar{x}}{2\sqrt{(1-\bar{x}^2)^2+b^2}} + \frac{\bar{x}}{2\sqrt{\bar{x}^2+b^2}},$$

$$g_2(\bar{x},\bar{x}_1) = \int_0^1 K(\bar{\xi},\bar{x})K(\bar{x}_1,\bar{\xi})\,d\bar{\xi}.$$

This provides an 'asymptotic' reflection equation that replaces (10), giving (correct to $O(\epsilon)$)

$$\rho c_p U\frac{\partial T}{\partial x} = \frac{\sigma\epsilon_f}{\delta}\left[T_{ht}^4 - 2T^4 + \frac{T_{hb}^4}{2}\left(\frac{L-x}{\sqrt{(L-x)^2+a^2}} + \frac{x}{\sqrt{x^2+a^2}}\right)\right] +$$

$$\frac{2\alpha(T)}{\delta}(T_g - T) + c\Delta HA\exp(-E_a/RT)$$

Figure 3 compares results produced by the full system (10)–(13) using 200 mesh points (bold line) and the asymptotic reflection model (broken line). Bearing in mind the fact that the small parameter ϵ in this case is only 0.08, the close agreement seems to indicate that the numerical method for solving the case when reflected radiation is included is giving accurate results. Some further numerical experiments employing larger numbers of mesh points and smaller values of ϵ confirmed the close agreement.

Figure 4 compares results for standard parameter values with (solid lines) and without reflected radiation (broken lines). The principal effect of the inclusion of reflected radiation is to slightly postpone the burning zone. The fabric temperature is also slightly reduced near to the furnace exit.

As a result of the computations described above, and from other cases that have been examined but not detailed, we draw the following conclusions.

(i) For the realistic range of constants discussed above, the amount of oil is reduced to the required level within the furnace as required.

(ii) Using the simpler model (no reflected radiation) an estimate of the width of the effective burning zone may be made by comparing results when the chemical-reaction term is respectively included and (incorrectly) excluded from the energy equation. When these results differ by more than 10 per cent in relative size, we assume that the burning zone has been reached. In the present case, this gives a burning zone extending from 0.25 to 0.32 m from the entrance to the furnace. When reflected radiation is included, the burning zone occupies the region 0.33–0.40 m. Granted, the figure of 10 per cent is arbitrarily chosen, but the burning zone thus predicted when reflected radiation is included agrees very closely with observations from the factory, providing yet further evidence that the model is giving accurate results. We further conclude that, in order to make qualitative predictions,

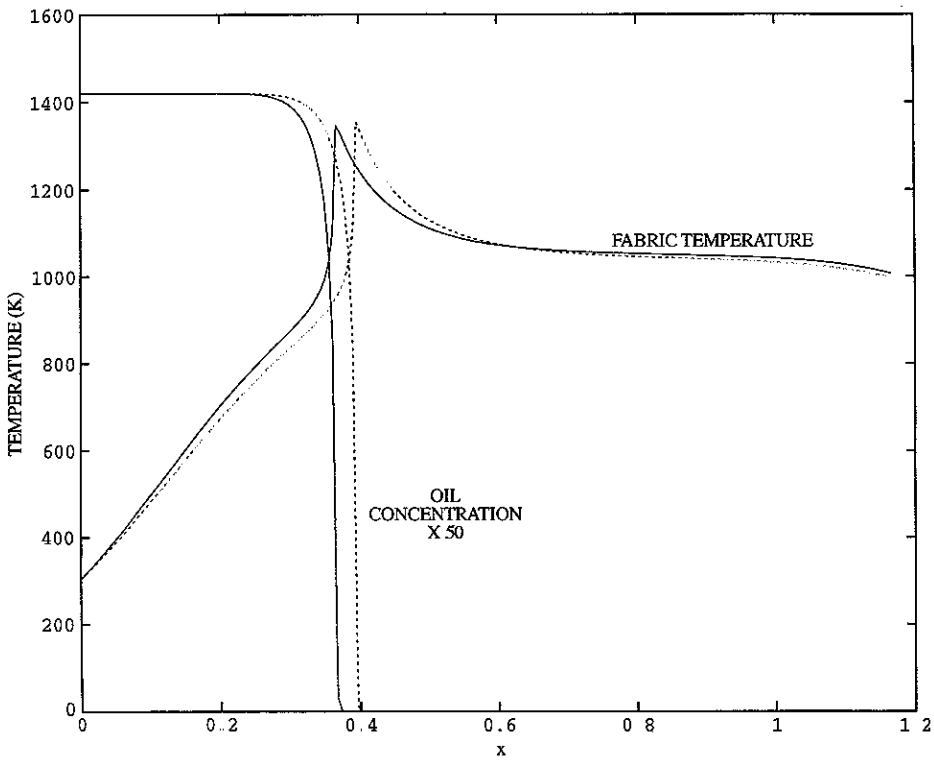

FIG 3 Comparison between full reflected radiation model (solid line) and 'asymptotic' reflected radiation model.

reflected radiation need not be included, and the simpler model may be used. If accurate predictions are required for the position of the burning zone, however, then reflected radiation must be included.

(iii) In almost all cases, the fabric temperature attains an almost constant value in the last half of the furnace before exit.

(iv) The simple model described above may be used to optimize the process; its accuracy and the value of its predictions will depend largely upon the availability of the relevant constants.

4. Modelling for thicker fabric sheets

In the models discussed above, the fabric sheet was so thin that the assumption that the temperature through a fabric sheet was effectively constant could be made With industrial applications in mind, it is worth pointing out that there may be other processes and products of a similar kind to those considered above where, although the fabric sheet is still thin compared to its length, its thickness is an order of magnitude greater. As well as considering thicker fabrics, the Valmiera factory may change other parameters in the manufacturing

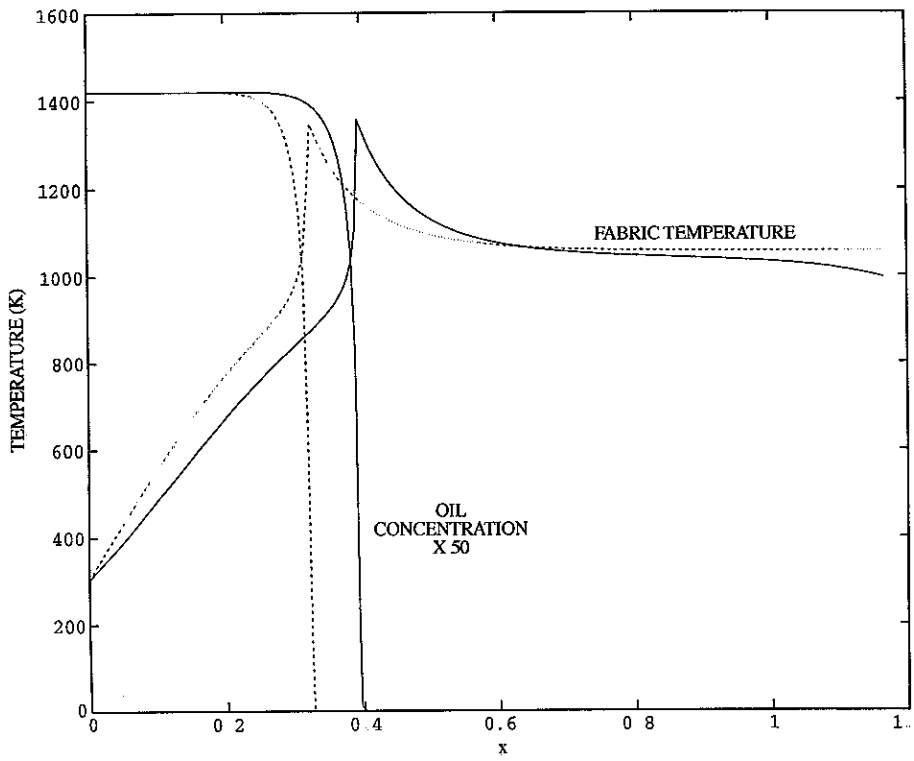

FIG 4. Comparison between models with (solid line) and without reflected radiation.

process (for example, by increasing the speed of the fabric) which would be equivalent to producing thicker fabrics.

In such cases, a different model is applicable. For reasons of brevity, we do not discuss fully the implications of thicker fabric sheets (a more complete analysis would have to address matters such as whether or not the oil concentration was a still a function of x alone, and what role was played by the various heating sources). Assuming simply that the temperature distribution in the fabric is now linear in y, we may write

$$\tilde{T}(x, y, t) = T(x, t) + \Delta T(x, t)(y - \delta/2).$$

With the effects of reflected radiation included, the model is now given by the equations

$$\rho c_p \left(\frac{\partial T}{\partial t} + U \frac{\partial T}{\partial x} \right) = k \frac{\partial^2 T}{\partial x^2} +$$

$$\frac{\epsilon_f}{\delta} \left[\sigma (T_{ht}^4 - (T + \Delta T \delta/2)^4) + \frac{1}{1 - \epsilon_f} (J_f - \sigma (T - \Delta T \delta/2)^4) \right] +$$

$$\frac{2\alpha}{\delta} (T_g - T) + c \Delta H A \exp(-E_a/RT),$$

$$J_f(x,t) = \epsilon_f \sigma (T(x,t) - \Delta T(x,t)\delta/2)^4 + (1-\epsilon_f)\int_0^L J_h(\xi,t)\frac{a^2}{2((\xi-x)^2+a^2)^{3/2}}\,d\xi,$$

$$J_h(x,t) = \epsilon_h \sigma T_{hb}^4 + (1-\epsilon_h)\int_0^L J_f(\xi,t)\frac{a^2}{2((\xi-x)^2+a^2)^{3/2}}\,d\xi,$$

$$\frac{\partial c}{\partial t} + U\frac{\partial c}{\partial x} = -cA\exp(-E_a/RT),$$

where ΔT is found via the boundary condition (3) to be

$$k\,\Delta\, T(x,t) = \epsilon_f \sigma [T_{ht}^4 - (T(x,t) + \Delta T(x,t)\delta/2)^4] +$$

$$\alpha(T + \Delta T\delta/2)[T_g - (T(x,t) + \Delta T(x,t)\delta/2)].$$

This problem may be solved in virtually the same manner as that described above, the only slight extra complication arising from the fact that ΔT is determined by a quartic equation. The problem for thicker fabric sheets may thus be addressed, though it will not be considered further here

5. Degradation of fabric strength

We have seen from the simple analysis presented above that the furnace provides sufficient heat to efficiently remove the necessary amount of oil from the fabric. Some attention must now be given to the main drawback in the procedure, namely the reduction of fabric strength that is associated with the heating and subsequent cooling process. For many hundreds of years it has been known that the properties of a solid glass sheet depend crucially upon the manner in which the molten product is cooled. In modern glass production the process of annealing, whereby the temperature of the cooling glass is strictly controlled, is necessary in order to prevent the creation of residual stresses that lead to fragile products. For high-quality optical glass, even more careful annealing is necessary as the refractive index is especially sensitive to cooling (for example, according to Jones (1971), the 200-inch mirror built for the Mount Palomar observatory was cooled from 500 to 300 degrees C at a rate of less than 1 degree C per day).

For the glass fabric under consideration, the main concern is the strength of the finished product. Many different models have been proposed for the calculation of transitory and residual stresses in glass, but the studies by Adams & Williamson (1920a,b) have come to be recognized as the first successful theoretical attempts to model the process of annealing. At high temperatures, it is assumed that the viscosity of the glass is such that thermal stresses may be instantly relieved, or at least, possess a relaxation time that is small compared to time scale of the annealing. Stresses are set up as the glass cools, and permanent stress distributions may be created as room temperature is approached.

The purpose of the present study is to examine simple improvements to the current glass fabric post-production process that will reduce the stresses set up in the glass as it

cools. To obtain accurate quantitative results is extremely hard; the prediction of permanent residual stresses has long been recognized to be a formidable problem. We therefore seek to establish a theory that gives qualitative results that nevertheless allow different cooling strategies to be compared. It will be noted below that the thin-layer theory that will be developed not only allows this, but may be generalized to allow for more involved effects; the complications involved are formidable however and the details will be postponed to subsequent studies.

The fact that both viscous and elastic effects are important in the glass solidification process has been recognized for many years (see, for example Narayanaswamy (1978)). A thermoviscoelastic model is thus required. We use the equations

$$k\nabla^2 T = \rho c_p \frac{dT}{dt} + mT_R \frac{de_{kk}}{dt}, \tag{14}$$

$$\frac{\partial \sigma_{ij}}{\partial x_j} + \rho b_i = \rho a_i,$$

$$\mathsf{P}_1 \sigma_{ij} = \mathsf{P}_2 e_{ij} + (K\mathsf{P}_1 - \mathsf{P}_2/3)\delta_{ij} e_{kk} - 3K\alpha_e \delta_{ij} \mathsf{P}_1 (T - T_R),$$

$$e_{ij} = \frac{1}{2}\left(\frac{\partial u_i}{\partial x_j} + \frac{\partial u_j}{\partial x_i}\right).$$

Here σ_{ij} is the stress tensor, e_{ij} the infinitesimal strain tensor, the u_i are the elastic displacements, b and a represent respectively the applied body forces and the acceleration, T_R is the reference state at which the material is stress-free, and $m = \alpha_e(3\lambda + 2\mu)$. As usual, λ and μ are the Lamé constants for the glass, whilst α_e denotes the coefficient of linear thermal expansion (dimensions K^{-1}). The differential operators P_1 and P_2 model the effects of viscoelasticity, while K is an elastic constant. Many choices are possible for both P_1 and P_2; in the current study we assume that a simple 'Maxwell body' model (see, for example, Boley & Weiner (1960)) is appropriate wherein

$$\mathsf{P}_1 = \frac{1}{2\mu}\frac{d}{dt} + \frac{1}{2\eta}, \qquad \mathsf{P}_2 = \frac{d}{dt},$$

and K, the bulk elastic modulus, is given by $K = \lambda + 2\mu/3$. In this formulation, the viscosity of the glass fabric is denoted by η, which is assumed to have dimensions of kg/m/sec. As usual, we consider the time-independent (steady-state operation) problem only, so $d/dt = U\partial/\partial x$.

As well as the assumption of small elastic displacements, this theory assumes that the temperatures are such that $(T - T_R)/T_R$ may be regarded as small. For glass, this is tantamount to the previous statement that the permanent stresses are set up only as a sample of fabric approaches room temperature. It is also worth bearing in mind that there is a little evidence to suggest that, for some kinds of glass, nonlinear elastic effects may be important. It is difficult to see how these could be included in any theoretical study, however, and such complications are therefore ignored.

Some discussion is also merited concerning whether or not the glass fabric behaves as an 'ordinary' thermoviscoelastic material. If the woven fabric fibres are effectively pinned at

the crossover points then thermally induced stresses could possibly be relieved by sliding. At the temperatures of interest, however, it seems unlikely that any sliding can take place. Examination of glass fibre samples (which we were able to briefly carry out in Riga) suggested that the fabric resembled a consolidated glass sheet to all intents and purposes, its only exceptional property being its flexibility at room temperature. The fabric weakening that concerned the manufacturers was, we were assured, essentially no different from that seen in ordinary sheets of glass. Accordingly no account has been taken of the behaviour of individual rods of which the fabric is composed.

Our first observation is that the coupling term $mT_R de_{kk}/dt$ in the temperature equation may be ignored. To see this, we compare kT_{yy} with $mT_R U \partial(e_{kk})/\partial x$. Using $m = \alpha_e(3\lambda + 2\mu)$, we find that scaling x_1 and x_2 with L and h respectively and using representative values $\alpha_e = 7 \times 10^{-6}/\mathrm{K}$, $\lambda = \mu = 2.4 \times 10^{10}\,\mathrm{N/m^2}$, the elastic displacement would need to have an order of magnitude of

$$u \sim \frac{kL^2}{h^2 \alpha_e U(3\lambda + 2\mu)} \sim 600\,\mathrm{m}$$

to contribute to the equations.

We now analyse the equations (14) in a thin layer of glass. Writing $u_1 = u$, $u_2 = v$, $x_1 = x$, and $x_2 = y$ for simplicity, we observe first that inertia may clearly be neglected. Also, gravity is unimportant, and thus body forces will be ignored. (Note: in this section we use a redefined y axis so that $y = 0$ is the plane of symmetry of the fabric. Inside the furnace, conditions are different at the top and bottom heaters. Outside the furnace, however, conditions are truly symmetrical. The variable x is now measured from the furnace exit.)

The problem that must be solved therefore amounts to

$$\frac{U}{2\mu}\frac{\partial \sigma_{ij}}{\partial x} + \frac{1}{2\eta}\sigma_{ij} = \Lambda_{ij}, \tag{15}$$

$$\operatorname{div} \sigma_{ij} = 0,$$

where

$$\Lambda_{ij} = U\frac{\partial e_{ij}}{\partial x} + \frac{(3\lambda + 2\mu)U}{6\mu}\frac{\partial e_{kk}}{\partial x}\delta_{ij} + \frac{(3\lambda + 2\mu)}{6\eta}e_{kk}\delta_{ij} - \frac{U}{3}\delta_{ij}\frac{\partial e_{kk}}{\partial x} -$$

$$(3\lambda + 2\mu)\alpha_e\left[\frac{U}{2\mu}\frac{\partial T}{\partial x} + \frac{(T - T_R)}{2\eta}\right]\delta_{ij}.$$

Here it has been assumed that $\eta = \eta(T(x, y))$ and, because of the decoupling of (14), the temperature has been calculated separately; the quantities λ, μ, and U are assumed to be constant. (Though the elastic constants vary with temperature, the dependence is exceedingly weak even over large ranges.) The thin glass sheet is assumed to be stress-free at $y = \pm h$, and to possess a given stress distribution σ_{ij0} as it exits from the furnace. (For our purposes, the uniformly heated nature of the fabric in the furnace means that we will normally assume that the fabric is stress-free upon exit from the furnace.) Solving (15), we find that

$$\sigma_{ij} = \frac{2\mu}{U}R(x, y)\int_0^x \Lambda_{ij}(\xi, y)R_1(\xi, y)\,d\xi + \sigma_{ij0}(y)\frac{R(x, y)}{R(0, y)}, \tag{16}$$

where

$$R(x, y) = \exp\left(\frac{-2\mu Q(x, y)}{U}\right), \qquad R_1(x, y) = \exp\left(\frac{2\mu Q(x, y)}{U}\right),$$

$$Q_x(x, y) = \frac{1}{2\eta(x, y)}.$$

We now subject the first equilibrium equation to a thin-layer analysis. Since the effects of introducing thin-layer scalings are rather obvious, we dispense with a rigorous non-dimensionalization of the equations. By scaling y and v with the small parameter $\epsilon = h/L$ and using (17), the first equilibrium equation (assuming $\sigma_{ij0} = 0$) becomes

$$\left[\frac{2\mu}{U}R(x, y)\int_0^x \Lambda_{11}(\xi, y)R_1(\xi, y)\,\mathrm{d}\xi\right]_x + \frac{1}{\epsilon}\left[\frac{2\mu}{U}R(x, y)\int_0^x \Lambda_{12}(\xi, y)R_1(\xi, y)\,\mathrm{d}\xi\right]_y = 0.$$

Inspection of the terms contained in elements of Λ shows that every term in Λ_{11} is order one in u, v, and their derivatives, while it is clear that in Λ_{12} the dominant term is u_{xy}, which is of order ϵ^{-1}. Thus, to leading order,

$$\left[R(x, y)\int_0^x u_{\xi y}(\xi, y)R_1(\xi, y)\,\mathrm{d}\xi\right]_y = 0. \tag{17}$$

We assume that this forces $u_{xyy} = 0$ By symmetry, this implies that

$$u_x(x, y) = A_0'(x),$$

so that, to leading order, the horizontal strains are functions of x alone. It is worth noting that there are alternatives to this assumption; for example, if $u_{xyy} = F(x)Q_{xy}$, where F is arbitrary, then (16) would also hold. Space does not permit a full discussion of these solutions, but they are not physically relevant and are therefore rejected.

Having effectively solved the first equilibrium equation to lowest order, we now turn to the second. Examination of the terms in the tensor Λ_{ij} shows that, when the variables are scaled, the equation becomes

$$\left[\frac{2\mu}{U}R(x, y)\int_0^x \Lambda_{22}(\xi, y)R_1(\xi, y)\,\mathrm{d}\xi\right]_y = 0$$

to lowest order. Using the fact that $\sigma_{22} = 0$ at $y = \pm h$, we conclude (using (15)) that $\Lambda_{22} = 0$ and thus, after simplification of Λ_{22},

$$v_{xy} + B_3(x, y)v_y = B_4(x, y),$$

where

$$B_3 = \frac{\mu(3\lambda + 2\mu)}{3\eta U(\lambda + 2\mu)},$$

$$B_4 = \frac{2\mu}{U(\lambda + 2\mu)}\left((3\lambda + 2\mu)\alpha_e\left[\frac{U}{2\mu}T_x + \frac{T - T_R}{2\eta}\right] - \frac{\lambda U}{2\mu}u_{xx} - \left(\frac{3\lambda + 2\mu}{6\eta}\right)u_x\right).$$

Setting $B_3(x, y) = B_{5x}(x, y)$, say, we find that

$$v_y = \mathrm{e}^{-B_5(x,y)} \int_0^x B_4(\xi, y)\mathrm{e}^{B_5(\xi,y)}\,\mathrm{d}\xi + v_{y0}(y)\exp(B_5(0, y) - B_5(x, y)). \tag{18}$$

This result allows the dominant stress σ_{11} to be determined. After some simplification, we find that

$$\Lambda_{11} = \frac{3\lambda + 2\mu}{\lambda + 2\mu}\left(\frac{\mu}{3\eta}v_y - \mu\alpha_e\left[\frac{U}{\mu}T_x + \frac{T - T_R}{\eta}\right] + \frac{\mu}{3\eta}A_0'\right) + \frac{2U(\lambda + \mu)}{(\lambda + 2\mu)}A_0''. \tag{19}$$

The stress in the glass sheet is thus determined using

$$\sigma_{11} = \frac{2\mu}{U}R(x, y)\int_0^x \Lambda_{11}(\xi, y)R_1(\xi, y)\,\mathrm{d}\xi + \sigma_{110}\frac{R(x, y)}{R(0, y)} \tag{20}$$

and all that remains is for the as yet unknown function $A_0' = u_x$ to be found.

A_0' may now be determined by assuming that, since there can be no net tension or compression acting upon the glass fabric sheet, the quantity

$$\int_{-h}^{h} \sigma_{11}\,\mathrm{d}y \tag{21}$$

must necessarily be zero. If the glass was being pulled with a net tension, (as in the process of glass fibre drawing, for instance) then naturally (21) could be assumed to be equal to the pulling tension. For the process discussed here, this tension is negligible compared to the stresses present in the glass. We shall also assume that this 'zero net tension' condition is equivalent to

$$\int_{-h}^{h} \Lambda_{11}\,\mathrm{d}y = 0, \tag{22}$$

and thus

$$\frac{\mu}{3}\int_{-h}^{h}\frac{v_y}{\eta(x, y)}\,\mathrm{d}y - B_7(x) + \frac{\mu}{3}A_0'(x)\int_{-h}^{h}\frac{\mathrm{d}y}{\eta(x, y)} + \frac{4hU(\lambda + \mu)}{(3\lambda + 2\mu)}A_0''(x) = 0, \tag{23}$$

where

$$B_7(x) = U\alpha_e\int_{-h}^{h} T_x(x, y)\,\mathrm{d}y - \mu\alpha_e\int_{-h}^{h}\frac{T(x, y) - T_R}{\eta(x, y)}\,\mathrm{d}y$$

It is worth mentioning that, on purely physical grounds, the truth of (22) seems plainly evident. Nevertheless, we have not been able to prove (22) rigorously from the zero-net-tension condition. If it was the case that η varied only slowly with T, then the near-independence of T on y would make η nearly independent of y, in which case (22) would follow from (21) on using (15). For molten glass, however, the strong dependence of the viscosity upon temperature rules out simple arguments of this type.

We may now use the expression (18) to show (the algebra is tedious but straightforward) that $A_0'(x)$ is determined by the integrodifferential equation

$$A_0''(x) + D_1(x)A_0'(x) + \int_0^x D_2(x, \xi)A_0''(\xi)\,\mathrm{d}\xi + \int_0^x D_3(x, \xi)A_0'(\xi)\,\mathrm{d}\xi + D_4(x) = 0, \tag{24}$$

where

$$D_1(x) = \frac{\mu(3\lambda + 2\mu)}{12hU(\lambda + \mu)} \int_{-h}^{h} \frac{dy}{\eta(x, y)},$$

$$D_2(x, \xi) = -\frac{\mu\lambda(3\lambda + 2\mu)}{12hU(\lambda + \mu)(\lambda + 2\mu)} \int_{-h}^{h} \frac{e^{-B_5(x,y)} e^{B_5(\xi,y)}}{\eta(x, y)} dy,$$

$$D_3(x, \xi) = -\frac{\mu^2(3\lambda + 2\mu)^2}{36hU^2(\lambda + \mu)(\lambda + 2\mu)} \int_{-h}^{h} \frac{e^{-B_5(x,y)} e^{B_5(\xi,y)}}{\eta(x, y)\eta(\xi, y)} dy,$$

$$D_4(x) = \frac{(3\lambda + 2\mu)}{4hU(\lambda + \mu)} \left[\frac{\mu}{3} B_9(x) - B_7(x)\right],$$

$$B_9(x) = \int_{-h}^{h} \frac{v_{y0}(y)}{\eta(x, y)} e^{B_5(0,y)} e^{-B_5(x,y)} dy +$$

$$\frac{E\alpha_e}{U(1 - \nu)} \int_{-h}^{h} \frac{1}{\eta(x, y)} e^{-B_5(x,y)} \int_0^x \left(\frac{U}{2\mu} T_\xi(\xi, y) + \frac{T(\xi, y) - T_R}{2\eta(\xi, y)}\right) e^{B_5(\xi,y)} d\xi\, dy.$$

In principle, the problem is now completely solved for arbitrary temperature distributions and viscosity–temperature relationships. The equation (24) is solved for $A_0'(x)$, this determines v_y from (23), and the stress $\sigma_{11}(x, y)$ is calculated using (19) in (20).

5.1 *Special cases of the general result*

The analysis above has shown that the complete problem may, at least in theory, be solved. The analysis involved for the most general case is formidable, however, and for the purposes of the present study we will be content to determine qualitative results by utilizing some special cases of the general theory.

Thermoelasticity in the limit $\eta \to \infty$. The pure thermoelastic problem may be examined by formally considering the limit $\eta \to \infty$. In this case $Q_x = 0$, and hence Q, and therefore R and R_1, are all constant. Thus (20) gives, for the case when there is no stress at $x = 0$,

$$\sigma_{11} = \frac{2\mu}{U} \int_0^x \Lambda_{11}(\xi, y)\, d\xi.$$

Assuming that $v_0(y) = 0$, we further find that $B_3 = B_5 = 0$. Using the definitions for B_4 and v_y in (19) shows that

$$\Lambda_{11} = \frac{U}{\lambda + 2\mu} \left[2(\lambda + \mu)A_0'' - \alpha_e(3\lambda + 2\mu)T_x\right],$$

where $A_0' = u_x$. Imposing the condition that

$$\int_{-h}^{h} \Lambda_{11}(x, y)\, dy = 0$$

now shows that

$$\Lambda_{11} = \frac{U\alpha_e(3\lambda+2\mu)}{\lambda+2\mu}\left[\frac{1}{2h}\int_{-h}^{h} T_x(x,y)\,dy - T_x(x,y)\right],$$

and, assuming that at $x = 0$ the glass sheet is completely stress-free and that the temperature is uniform as a result of the furnace heating, we find that

$$\sigma_{11} = \frac{E\alpha_e}{1-\nu}\left[\frac{1}{h}\int_0^h T(x,y)\,dy - T(x,y)\right], \tag{25}$$

where $E = (3\lambda+2\mu)\mu/(\lambda+\mu)$ and $\nu = \lambda/2(\lambda+\mu)$ are Young's modulus and Poisson's ratio respectively

The expression (25) has been derived before (see, for example Adams & Williamson (1920a,b) and Guillemet (1990)). For a typical temperature profile in the current case, where the glass fabric sheet is hottest at its centre and is cooled rapidly at its surface, (25) predicts, as might be expected, $\sigma_{11} < 0$ (compression) near the centre of the sheet $y = 0$ and $\sigma_{11} > 0$ (tension) near the surfaces of the sheet. Although (25) may, for a given temperature field, provide approximate results for the evolution of the tension and compression within a glass fabric sheet, it is clear that, when the cooling process is finished and the sheet is uniformly at room temperature, the stress given by (25) must be zero. Such a simple model is therefore quite incapable of predicting permanent stresses.

The simplicity of the formula (25) is appealing, and because of this attempts have been made to modify it in ways that allow the prediction of permanent stresses. Bartenev (1948) suggested that (25) be modified to read

$$\sigma_{11} = \frac{E\alpha_e}{1-\nu}\left[\frac{1}{h}\int_0^h \Phi(x,y)\,dy - \Phi(x,y)\right],$$

where

$$\frac{d\Phi}{dx} = \left[\frac{dT}{dx}\right]_{T=T_{gf}}$$

and T_{gf} is the 'glass freezing' temperature. Although this modification (and others) have given results consistent with experiments in some instances, in other cases agreement has been poor. Such models must clearly be regarded as unsatisfactory in that they neglect the viscosity of the glass. Since the strong dependence of this quantity upon temperature is one of the principal reasons why permanent stresses may be created, some attempt must be made to include flow effects into the stress model.

Thermoviscoelasticity with constant viscosity. The case where viscoelastic effects are included may also be dealt with relatively easily when the viscosity η is constant. Using the theory developed above, we find that in this case

$$\Lambda_{11} = \frac{\mu(3\lambda+2\mu)}{3\eta(\lambda+2\mu)}\left[e^{-B_5(x)}\int_0^x B_4(\xi,y)e^{B_5(\xi)}\,d\xi\right] - \frac{2\mu\alpha_e(3\lambda+2\mu)}{(\lambda+2\mu)}T^* +$$

$$\frac{1}{\lambda+2\mu}\left(\frac{\mu}{3\eta}(3\lambda+2\mu)A_0' + 2U(\lambda+\mu)A_0''\right),$$

where

$$B_5(x) = \frac{\mu(3\lambda + 2\mu)x}{3\eta U(\lambda + 2\mu)},$$

$$B_4(x, y) = \frac{2\mu}{U(\lambda + 2\mu)}\left[(3\lambda + 2\mu)\alpha_e T^* - \frac{\lambda U}{2\mu}A_0'' - \left(\frac{3\lambda + 2\mu}{6\eta}\right)A_0'\right],$$

$$T^*(x, y) = \frac{U}{2\mu}T_x + \frac{1}{2\eta}(T - T_R),$$

and $A_0' = u_x$. The function A_0' may be determined in the usual way by insisting that

$$\int_{-h}^{h} \Lambda_{11}(x, y)\,dy = 0.$$

This gives

$$\Lambda_{11} = \frac{\alpha_e E^2}{6U\eta(1-\nu)^2}e^{-B_5(x)}\int_0^x e^{B_5(\xi)}\left[T^*(\xi, y) - \frac{1}{2h}\int_{-h}^{h} T^*(\xi, y)\,dy\right]d\xi +$$

$$\frac{E\alpha_e}{1-\nu}\left[\frac{1}{2h}\int_{-h}^{h} T^*(x, y)\,dy - T^*(x, y)\right],$$

so that finally

$$\sigma_{11} = \frac{2\mu}{U}\exp\left(-\frac{\mu x}{U\eta}\right)\int_0^x \Lambda_{11}(\xi, y)\exp\left(\frac{\mu\xi}{U\eta}\right)d\xi, \tag{26}$$

where Λ_{11} and T^* are as given above. This result does not appear to have arisen in the literature before, and we use it to make comparisons of various cooling schedules below. The expression (26) provides a complete solution for the thermoviscoelastic stresses in the constant viscosity thin-layer problem, and may therefore be regarded as a generalization of (25). Although use will be made of this expression to predict stresses during cooling, we note that (26) suffers from an identical limitation to that of the formula (25), namely an inability to predict *permanent* stresses. To see this, we note that, whatever the structure of Λ_{11}, the solution of (15) will be given, in the constant-viscosity case, by (26). Because of the total-stress condition that has been imposed upon σ_{11}, it is inevitable that $\Lambda_{11} \to 0$ as $x \to \infty$. The negative exponential in (26) therefore ensures that σ_{11} will decrease to zero as $x \to \infty$.

On physical grounds, this conclusion is not surprising. We may expect that, in order to create permanent stresses, changes in viscosity are necessary. A brief examination of the paradigm problem

$$\frac{d\sigma(x)}{dx} + f(x)\sigma(x) = g(x),$$

where $g(x) \to 0$ as $x \to \infty$, shows that, for constant $f(x) \geqslant 0$, it must be the case that $\sigma(x) \to 0$ as $x \to \infty$. If $f(x) \to 0$ faster than $1/x$, however, then it is easy to see that, when (say) $g(x)$ is a negative exponential, solutions where σ is finite at ∞ are possible.

Thermoviscoelasticity with temperature-dependent viscosity. Although, as noted above, the problem may be solved for a fully temperature-dependent viscosity, the associated integral equation must be solved numerically. The details are complicated and the resulting stress formulae are most unwieldy. For practical purposes, a compromise may be made by assuming that the viscosity, though temperature-dependent, depends only upon x. The asymptotic temperature distributions that will be derived below for the glass fabric after it leaves the furnace confirm that this is an extremely good approximation for all but the smallest values of x.

With this assumption, the derivation of a formula for the stresses is similar to the case considered above, but now (assuming $v_{y0}(y) = 0$) we have

$$v_y = \mathrm{e}^{-B_5(x)} \int_0^x B_4(\xi, y)\mathrm{e}^{B_5(\xi)}\,\mathrm{d}\xi,$$

where

$$B_5(x) = \frac{\mu(3\lambda + 2\mu)}{3U(\lambda + 2\mu)} \int_0^x \frac{\mathrm{d}\xi}{\eta(\xi)},$$

$$B_4(x, y) = \frac{2\mu}{U(\lambda + 2\mu)} \left[(3\lambda + 2\mu)\alpha_\mathrm{e} T^* - \frac{\lambda U}{2\mu} A_0'' - \left(\frac{3\lambda + 2\mu}{6\eta(x)} \right) A_0' \right],$$

$$T^*(x, y) = \frac{U}{2\mu} T_x + \frac{1}{2\eta(x)} (T - T_\mathrm{R})$$

The final expressions for the stress are then given by

$$\Lambda_{11}(x, y) = \frac{E^2 \alpha_\mathrm{e}}{6U\eta(x)(1 - \nu)^2} \mathrm{e}^{-B_5(x)} \int_0^x \mathrm{e}^{B_5(\xi)} \left[T^*(\xi, y) - \frac{1}{2h} \int_{-h}^{h} T^*(\xi, y)\,\mathrm{d}y \right] \mathrm{d}\xi +$$

$$\frac{E\alpha_\mathrm{e}}{1 - \nu} \left[\frac{1}{2h} \int_{-h}^{h} T^*(x, y)\,\mathrm{d}y - T^*(x, y) \right],$$

$$\sigma_{11} = \frac{2\mu}{U} \exp\left(\frac{-2\mu Q(x)}{U} \right) \int_0^x \Lambda_{11}(\xi, y) \exp\left(\frac{2\mu Q(\xi)}{U} \right) \mathrm{d}\xi, \tag{27}$$

where

$$Q_x(x) = \frac{1}{2\eta(x)}.$$

The expression (27) may be evaluated without too much difficulty to determine the stresses when the viscosity is a given function of x; it is worth pointing out, however, that for a typical exponential viscosity (such as the one used below) some care is required if the integrals are to be evaluated accurately.

6. Determination of the temperature distribution in the fabric

The stress calculations discussed above assume that the temperature in the fabric is known To determine T, a number of assumptions must be made concerning the nature of the cooling experienced by the glass fabric as it leaves the furnace. Although many different regimes are possible, two cooling programmes are discussed below.

6.1 *Cooling from room temperature*

The simplest (but crudest) model for the cooling of the glass fabric assumes that the fabric emerges from the furnace at a temperature T_a (which we expect to be close to, but not necessarily equal to, T_f) into an environment which is largely at room temperature T_b. Some explanation of the assumptions that will be made is helpful: because of heat losses from the gap in the furnace through which the glass exits, it is inaccurate to make the simple assumption that $T = T_b$ immediately upon exit from the furnace. Instead, we assume that the ambient temperature is given by

$$T = T_b - (T_b - T_a)e^{-k_c x/L_c}, \tag{28}$$

where $k_c \gg 1$ and L_c is a length scale to be defined. The cooling problem in the glass, assuming Newton cooling at the surfaces of the sheet, is thus

$$\rho c_p U T_x = k(T_{xx} + T_{yy})$$

with

$$T = T_a \quad (x = 0), \qquad T_y = 0 \quad (y = 0),$$

and

$$T_y = \bar{\beta}(T - T_b - (T_a - T_b)e^{-k_c x/L_c}) \quad (y = h),$$

where $\bar{\beta}$ (units m^{-1}) is a heat transfer coefficient. By non-dimensionalizing by setting $x = L_c\bar{x}$, $y = h\bar{y}$ and $T = T_b + \psi(T_a - T_b)$ and immediately dropping the bars for convenience, the problem to be solved is

$$\psi_x = \frac{L_c k}{\rho c_p U h^2}\left(\frac{h^2}{L_c^2}\psi_{xx} + \psi_{yy}\right)$$

with

$$\psi = 1 \quad (x = 0), \qquad \psi_y = 0 \quad (y = 0),$$

and

$$\psi_y = h\bar{\beta}(\psi - e^{-k_c x}) \quad (y = 1)$$

Examining the sizes of the non-dimensional parameters involved, we find that (using standard values and $L_c = 0.6$—the latter value for reasons that will be explained below)

$$\frac{L_c k}{\rho c_p U h^2} \sim 330 \sim \frac{1}{\epsilon} \quad \text{(say)},$$

thus defining a small parameter ϵ, while

$$h\bar{\beta} = 10^{-4}\bar{\beta} = q\epsilon,$$

where $q < 0$ is O(1). By ignoring the term multiplied by h^2/L_c^2, the equation may therefore be cast in the form of a perturbation problem by writing

$$\epsilon\psi_x = \psi_{yy}, \qquad \psi_y = q\epsilon(\psi - e^{-k_c x}) \quad \text{at } y = 1.$$

Seeking a regular perturbation solution $\psi(x, y) = A_0(x) + \epsilon A_1(x, y) + \epsilon^2 A_2(x, y) + \ldots$, we find that

$$A_0 = \frac{q e^{-k_c x} + k_c e^{qx}}{q + k_c},$$

$$A_1 = \frac{y^2 k_c q (e^{qx} - e^{-k_c x})}{2(q + k_c)} + \frac{qx}{6(q + k_c)^2}\left[e^{-k_c x}(3q + k_c) + e^{qx}(2xq^2 + 2xk_c q - 3q - k_c)\right].$$

To derive these solutions, use has been made of the fact that $\psi = 1$ at $x = 0$. For small x, the term ψ_{xx} cannot be ignored, and a boundary layer is present. However, analysis shows that the outer limit of the inner solution is simply $\psi = 1$. In dimensional variables, therefore,

$$T = T_b + (T_a - T_b)\left[\frac{q e^{-kx/L_c} + k e^{qx/L_c}}{q + k} + \epsilon\left(\frac{kqy^2}{2h^2(k + q)}(e^{qx/L_c} - e^{-kx/L_c}) + \right.\right.$$

$$\left.\left.\frac{qx}{6L_c^2(q + k)^2}(L_c(k + 3q)(e^{-kx/L_c} - e^{qx/L_c}) + 2xq(q + k)e^{qx/L_c})\right)\right]. \qquad (29)$$

It is worth noting that, when the ψ_{xx} term is neglected, the equations may be solved for arbitrary ϵ by transform methods. Although the method is elementary, the resulting solution is unwieldy. The full problem may also be solved numerically with little difficulty using standard methods. Some simple comparisons show that (29) provides an extremely accurate approximation to the exact solution for all but the smallest values of x.

6.2 *Amelioration of cooling by the insertion of metal plates*

As will be seen in the next section, the stresses that result from plain Newton cooling as described above are unacceptably high, and lead to a product that is of a lower quality than that desired. Obviously the quality will be improved if the cooling can be performed more slowly. One cost-effective way to do this (the economic constraints of the factory render it essential that no extra expense is incurred, so that the addition of elaborate heating fans and the like is not a realistic option) is to attach metal plates in contact with the top and bottom heaters that extend past the foundation bricks outside the furnace. This effectively shields the glass fabric from the ambient conditions outside. Experiments carried out at the factory have shown that to a good approximation the metal plates may be assumed to produce an effective linear ambient temperature distribution. As far as the fabric is concerned, therefore, at $x = 0$ the ambient temperature is T_a, while the ambient temperature has dropped linearly to T_b by the time the fabric comes into contact with the first downstream roller ($x \sim 60$ cm).

Proceeding using the same degrees of approximation as for the Newton cooling case considered above, we find that the equivalent formula to (29) is

$$T = T_b + (T_a - T_b)\left[1 - \frac{x}{L_c} + \frac{1}{q}\left\{\exp\left(\frac{qx}{L_c}\right) - 1\right\} + \epsilon\left\{\left(\exp\left(\frac{qx}{L_c}\right) - 1\right)\left(\frac{y^2}{2h^2} - \frac{1}{2}\right) + \right.\right.$$

$$\left.\left.\frac{qx}{3L_c}\exp\left(\frac{qx}{L_c}\right)\right\}\right]. \qquad (30)$$

Once again, the problem may be solved in closed form in an elementary manner using Laplace transforms. However, the solution is unwieldy and complicated. It may easily be confirmed that (30) provides exceedingly accurate approximations even a few millimetres away from $x = 0$.

7. Stress predictions for different cooling regimes

Now that the temperature distribution in the cooling glass is known to a good degree of approximation, stress predictions may be made using (25), (26), and (27). A key component of the prediction method when fluidity effects are taken into account is the provision of a suitable viscosity law for the glass. Detailed viscosity experiments have not been carried out by the Valmiera factory, and so we must rely upon values given in the literature for 'similar' products. Inevitably this will involve the use of some sort of average; for the results shown below we have used a combination of various laws proposed by Bansal & Doremus (1986) for the viscosity of KG-33 Borosilicate, EZ-I Aluminosilicate, KG-I Alkali–lead, and R-6 Soda–Lime. The formula used is

$$\eta = 0.138 \times 10^{-17} \exp\left(\frac{58902}{T}\right), \tag{31}$$

where η is measured in Pa s and T in K. Without detailed experiments, an average of this sort is probably the only practical way of proceeding, but a glance at the coefficient and exponent used in (31) confirms that extreme sensitivity to temperature is present. Because of this dependence, separate results (not shown below) were also calculated using different viscosity laws. In each case the magnitudes of the predicted stresses varied (in some cases by fairly large amounts) but the trends and general conclusions suggested by the results given below were confirmed. It is also worth pointing out that, as might be expected, (31) is an 'Arrhenius'-type formula. It is therefore possible that the stress formulae may be further simplified by using high-activation-energy asymptotics. This approach has not been pursued in the present work.

A brief comment is necessary concerning the value of k_c, whose reciprocal characterizes the distance over which the ambient temperature outside the furnace is influenced by heat escaping from the furnace. A number of results were computed for various different values of k_c. They were virtually identical for all k_c that exceeded about 50, thereby confirming observations from the factory that the region of influence is very small. For all the results computed below, a value of $k_c = 100$ was therefore used.

The only other 'experimental' parameter that needs to be prescribed before stress calculations can be made is the heat-transfer coefficient q. No experimental data are available from the factory and it is evident that—since, in reality, q probably has to represent the effects of laminar, transitional, and turbulent free and forced convection effects—theoretical attempts to determine values for it are likely to be doomed to failure. Various estimates are recommended in the literature, most sources simply citing a range of possible values. Holman (1976) is typical, indicating that q lies in the range $-20 < q < -1/3$ for 'forced air convective cooling'; other similar heat-transfer texts give comparable but varying values. Accordingly, the results documented below have been calculated using values of q such as -1 and -5. Further results given in Fig. 7 confirm that the general conclusions regarding the effect of adding metal plates to the process remain unaltered as q is varied.

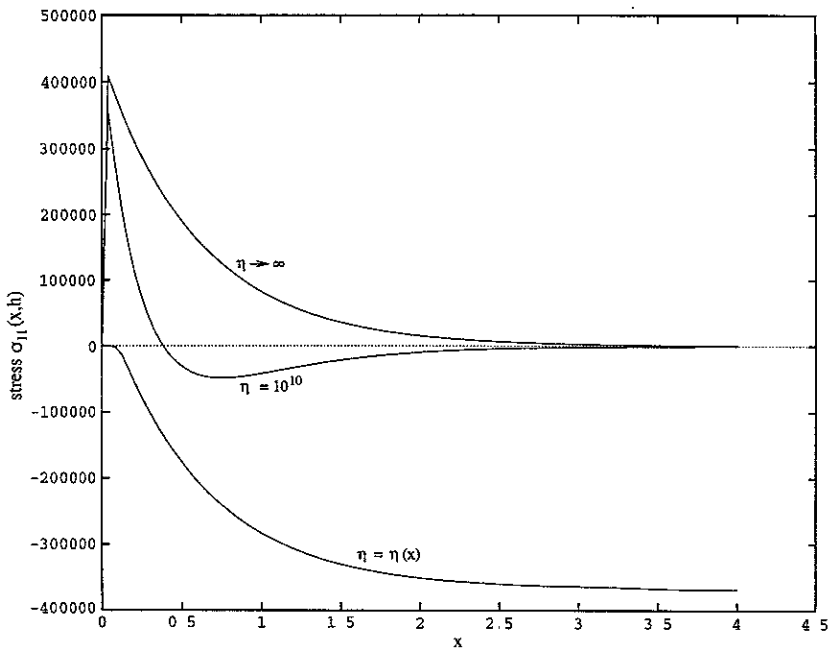

FIG 5. Surface stresses for Newton cooling for infinite-viscosity, finite-constant-viscosity, and temperature-dependent-viscosity models.

For each of the sets of results shown below, only the surface stress has been displayed. Examination of each of the formulae (25), (26), and (27) reveals that, because of the definition of T^*, the centreline stress may be calculated simply by multiplying the surface stress by a factor of $-1/2$.

Figure 5 shows three sets of results which are indicative of the sort of predictions that the simplified models are capable of. In each case the surface stress $\sigma_{11}(x, h)$ is shown for the Newton cooling regime where the ambient temperature is given by (28) Values of $k_c = 100$ and $q = -1$ were used. It is generally accepted in the glass processing industry that Newton cooling of a thin glass sheet carried out in this fashion nearly always results in a product that carries a permanent surface compression and centre tension. For the simple thermoelastic model ($\eta \to \infty$) where the stresses are given by (25), not only is no permanent stress predicted, but the signs of the transient stresses are incorrect, casting serious doubts on the ability of (25) (in spite of its popularity and wide usage) to produce any useful results. Matters are improved when a viscoelastic formulation with a constant viscosity (in this case $\eta = 10^{10}$) is used. After a high initial surface tension (inevitable as the constant-viscosity model is unable to take the increased fluidity of the glass soon after the furnace exit into account), a surface compression is correctly predicted—though, as pointed out above, no permanent stress can exist. When the effects of variable viscosity (defined by (31)) are included, the initial fluidity of the glass prevents high stresses developing by allowing them to equalize through flow. As room temperature is neared, the rapidly increasing viscosity acts to 'lock in' a surface compression and centre tension, and

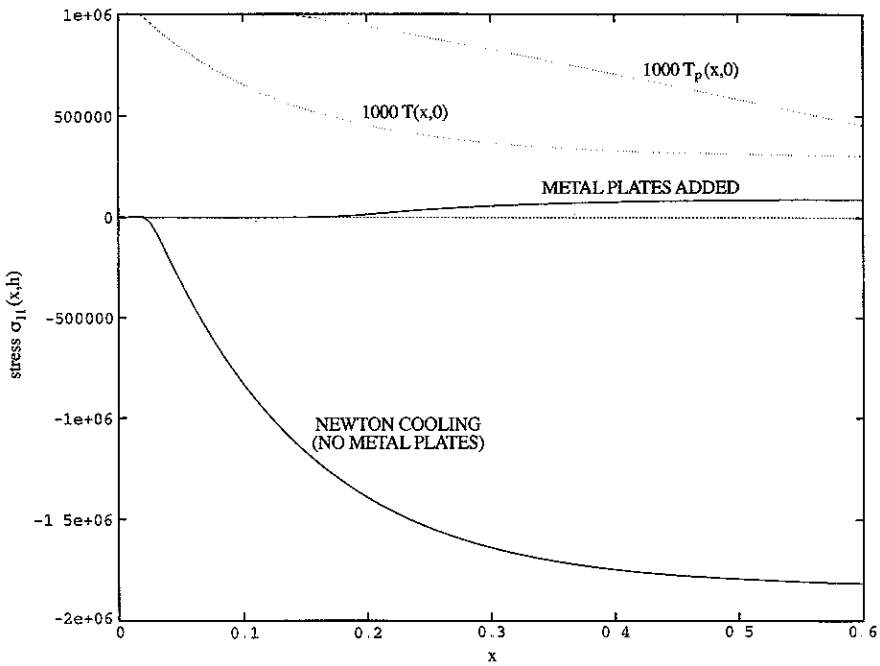

FIG 6. Surface stresses and fabric centre temperatures with and without metal plates ($q = -5$, temperature-dependent viscosity)

a permanent stress distribution is set up. We conclude that the inclusion of temperature-dependent viscosity effects is crucial.

In Fig. 6, the surface stresses predicted by (27) with the temperature-dependent viscosity given by (31) are compared for Newton cooling and the case with added metal plates. Values of $k_c = 100$ and $q = -5$ were used, and we note that with these values it is clear that the permanent stress distribution in the fabric has reached an amount very close to its final value by the time the fabric crosses the rollers at $x = L_c$. Striking differences between the two cases are also visible: Newton cooling, as expected, produces a surface compression, while a surface tension in the glass is produced when metal plates are added. However, the magnitude of the tension produced in the latter case is substantially less than for Newton cooling, suggesting that the addition of metal plates is likely to prove extremely beneficial to the manufacturing process as a whole. Figure 6 also shows the fabric centreline temperatures (broken lines) for comparison, the slower fall of the temperature distribution $T_p(x, 0)$ when metal plates are included being clear.

In Fig. 7, results are presented for the case where metal plates are added (the data being identical to those used for Fig 6) using the stress predictions (25), (26), and (27). The failure of the simpler models to accurately predict the stresses, especially at the start of the cooling process, is again apparent. Although (perhaps fortuitously) the constant viscosity model gives a similar value for the surface tension force at $x = L_c$, the simple thermoelastic model once again produces predictions that are unacceptably in error.

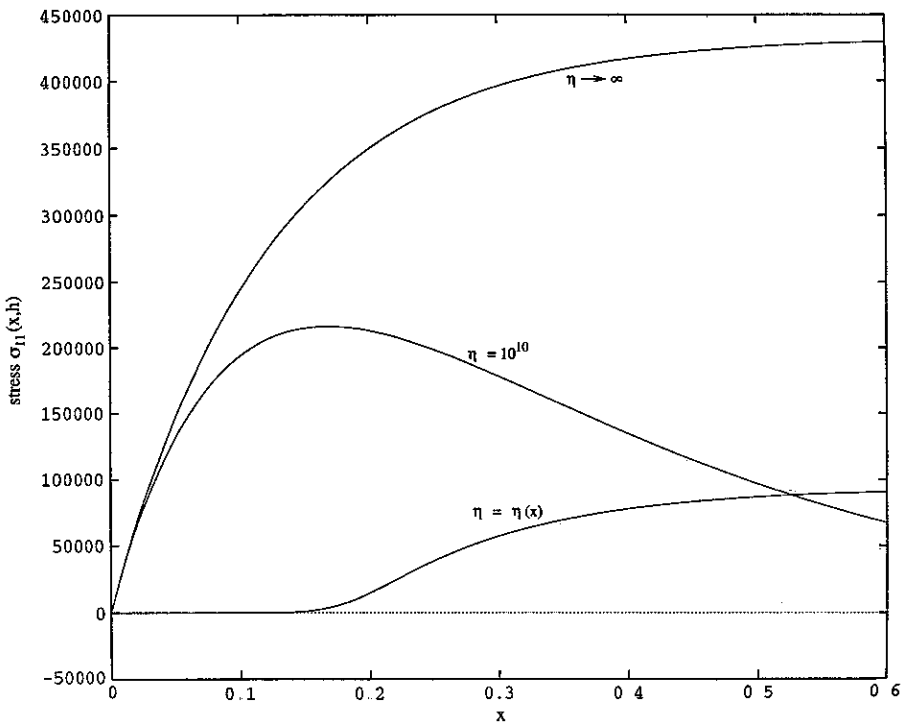

FIG. 7 Surface stresses predicted by constant-viscosity, infinite-viscosity, and temperature-dependent-viscosity models for cooling with metal plates ($q = -5$).

Finally, the results given in the table below show that the results in Fig. 6 are typical of a general trend. Table 1 shows surface stresses with and without metal plates for $k_c = 100$ and various different values of the heat transfer coefficient q, the calculations having been made with the temperature-dependent viscosity model.
In each case, the introduction of metal plates leads to a significant reduction in stress; for higher values of the heat-transfer coefficient, the stress is reduced by an order of magnitude. Though space constraints do not permit their inclusion, many more comparisons of this sort were carried out, each leading to similar conclusions. The overall verdict regarding the introduction of metal plates must therefore be as follows.

(i) The introduction of metal plates will lead to a significant reduction in the permanent stresses produced in the glass fabric It is worth mentioning that, during the course of this theoretical study, the factory has actually fitted metal plates of the form described above. Though it is too early to tell whether product quality has been greatly enhanced, such an improvement is anticipated.

(ii) The resultant product is likely to possess a surface tension as opposed to a surface compression which would arise from pure Newton cooling.

As well as these conclusions, it has become evident that, to make reliable predictions of

TABLE 1

q	$\sigma_{11}(0.6, h)$ (no plates)	$\sigma_{11}(0.6, h)$ (metal plates)	|stress ratio|
−0.4	−0.269E5	0.584E4	4.64
−0.6	−0.736E5	0.292E5	2.52
−0.8	−1.342E5	0.521E5	2.58
−1.0	−2.048E5	0.708E5	2.89
−2.0	−6.242E5	1.150E5	5.43
−3.0	−10.549E5	1.166E5	9.05
−4.0	−14.530E5	1.048E5	13.86
−5.0	−18.140E5	0.905E5	20.04
−10.0	−32.562E5	0.407E5	80.00

either transitory or permanent stresses in cooling or annealing glass, it is essential that thermal, viscous, and elastic effects are all included. Moreover, any successful model must take fully into account the highly temperature-dependent nature of the viscosity of glass.

Acknowledgement

The collaboration that led to this study was made possible by ECMI (the European Consortium for Mathematics in Industry). The authors are also grateful to Dr. Patrick Hendra of the University of Southampton for assistance in determining the chemical properties of polymers.

A. Nomenclature table and physical constants

Where possible, typical values of the constants are given. Unless otherwise specified, these are used in the text.

A Pre-exponential Arrhenius constant ($= 1.0 \times 10^9$/sec)
a Distance between fabric and bottom heater ($= 150$ mm)
$\boldsymbol{a}$ Acceleration
$\boldsymbol{b}$ Body force
c Concentration of oil in fabric (mol/m^3)
c_0 Initial oil concentration in fabric ($= 28.387$ mol/m^3)
c_p Fabric specific heat ($= 690.82$ J/kg/K)
D Width of fabric sheet ($= 1.1$ m)
e_{ij} Infinitesimal strain tensor
E Young's modulus $= \mu(3\lambda + 2\mu)/(\lambda + \mu)$
E_a Activation energy of oil ($= 160$ kJ/mol)
g Gravitational acceleration (9.81 m/sec^2)
G_f Irradiation of fabric bottom surface
G_h Irradiation of bottom heater
h Semi-thickness of fabric $= \delta/2$ ($= 0.1$ mm)

ΔH Heat of reaction of oil ($= 1.207 \times 10^7$ J/mol)
J Radiosity of fabric surface
J_f Radiosity from the bottom surface of fabric
J_h Radiosity from bottom heater
K Elastic constant $\lambda + 2\mu/3$
k Fabric thermal conductivity ($= 1.38$ W/m/K)
k_c Non-dimensional constant for furnace exit heat losses
k_g Gas thermal conductivity (~ 0.0669 W/m/K)
k_o Thermal conductivity of oil (W/m/K)
L Length of heated part of furnace ($= 1.166$ m)
L_c Length of cooling region outside furnace ($= 0.6$ m)
m Thermal expansion constant $\alpha_e(3\lambda + 2\mu)$
Q_f Net energy leaving fabric bottom surface
r_f Reflectivity coefficient of fabric bottom surface
R Gas constant ($= 8.31441$ J/K/mol)
Re Reynolds number $= LU_g/\nu_g$
T y-averaged temperature in fabric
$\tilde{T}$ Temperature in fabric (before averaging)
T_a Room temperature outside the furnace
T_b Final exit temperature of glass from furnace
T_f Final fabric temperature in furnace
T_g Temperature of gas in furnace
T_{gf} Glass freezing temperature
T_{hb} Temperature of bottom heater ($= 1123$ K)
T_{ht} Temperature of top heater ($= 973$ K)
T_{io} Ignition temperature of oil ($= 693$ K)
T_0 Initial fabric temperature ($= 303$ K)
T_R Reference temperature at which glass is stress-free (K)
U Fabric speed in furnace ($= 0.33$ m/sec)
U_g Air speed ($= 0.33$ m/sec)
V Typical flow velocity of molten glass
α $\mathrm{Nu}k_g/\mathrm{L}$ = Convective heat transfer coefficient (~ 1.3 W/m^2/K)
α_e Glass coefficient of linear expansion ($= 7 \times 10^{-6}$/K)
$\bar{\beta}$ Heat transfer coefficient for glass cooling (m^{-1})
δ Fabric thickness ($= 0.2$ mm)
ϵ Small parameter (may be different in different sections)
ϵ_f Fabric emissivity ($= 0.92$)
ϵ_h Bottom heater emissivity ($= 0\ 8$)
η Glass dynamic viscosity (kg/m/sec)
λ Lamé constant
μ Lamé constant
ν Poisson's ratio $\lambda/2(\lambda + \mu)$ ($= 0.25$)
ν_g Gas kinematic viscosity ($= 1.2 \times 10^{-4}$ m^2/sec)
ρ Fabric density ($= 1100$ kg/m^3)
ρ_o Oil density ($= 1100$ kg/m^3)

σ Stefan–Boltzmann constant ($= 5.6703 \times 10^{-8}$ W/m^2/K^4)
σ_{ij} Stress tensor in glass
θ Non-dimensional averaged temperature in fabric sheet

REFERENCES

ADAMS, L. H., & WILLIAMSON, E. D. 1920a The annealing of glass. *J. Franklin Inst.* **190**, 597–631.
ADAMS, L. H., & WILLIAMSON, E. D. 1920b The annealing of glass. *J. Franklin Inst.* **190**, 835–870.
BANSAL, N. P., & DOREMUS, R. H. 1986 *Handbook of glass properties*. Academic Press, New York.
BARTENEV, G. M. 1948 (In Russian). *Dokl. Akad. Nauk. SSSR* **60**, 257–278.
BOLEY, B. A., & WEINER, J. H. 1960 *Theory of thermal stresses*. John Wiley & Sons, New York.
BRANDRUP, J., IMMERGUT, E. H., & MCDOWELL, W. 1975 *Polymer handbook*. Wiley-Interscience, New York.
BUIKIS, A., FITT, A. D., & ULANOVA, N. 1997 A model of oil burnout from glass fabric. *Proceedings of the 9th ECMI Conference*, Lyngby, 1996.
GUILLEMET, C. 1990 Annealing and tempering of glass. *J. Non-crystalline Solids* **123**, 415–426.
HALL, G., & WATT, J. M. 1976 *Modern numerical methods for ordinary differential equations*. Clarendon Press, Oxford.
HOLMAN, J. P. 1976 *Heat transfer* (4th edn). McGraw-Hill, New York.
JONES, G. O. 1971 *Glass*. Chapman & Hall.
MIHEEV, M. A. 1940 *Heat transfer*. Energy Publishing House, Moscow (in Russian).
NARAYANASWAMY, O. S. 1978 Dehydration behaviour of aluminium sulfate hydrates. *J. Am. Ceram. Soc.* **61**, 146–152.
SIEGEL, R., & HOWELL, J. R. 1972 *Thermal radiation heat transfer*. McGraw-Hill, New York.